MITT.ÖSTERR.MINER.GES. 156 (2010)

MULTI-EQUILIBRIUM- AND PSEUDOSECTION MODELLING OF THE NORTHERNMOST SOUTHALPINE BASEMENT (BRIXEN QUARTZPHYLLITE, SOUTH-TYROL, ITALY)

by

Stefan Wyhlidal[1*], Werner F. Thöny[1], Peter Tropper[1] & Volkmar Mair[2]

[1*]AIT, Austrian Institute of Technology
A-2444 Seibersdorf, Austria
[1]Institute of Mineralogy and Petrography
University of Innsbruck, Innrain 52, A-6020 Innsbruck, Austria
[2]Amt für Geologie und Baustoffprüfung
Eggentalerstrasse 48, I-39053 Kardaun (BZ), Italy

Abstract

The northernmost Southalpine basement rocks, the Brixen quartzphyllites, which lack a Permian contact metamorphic overprint, were sampled near Waidbruck/Ponte Gardena and Spiluck/Spelonca in South-Tyrol, Italy. These samples contain the mineral assemblage muscovite + chlorite + albite + biotite + garnet + quartz ± K-feldspar. This mineral assemblage represents the Variscan peak metamorphic assemblage of the Southalpine basement and yields maximum P-T conditions of 0.53–0.59 GPa and 521–551°C using multi-equilibrium calculation thermobarometry using the software THERMOCALC v.3.23. Pseudosection modelling using the software THERIAK–DOMINO was done using XRF bulk rock analyses of the samples. The obtained P-T data using the multi-equilibrium approach are slightly higher but still in very good agreement with the Variscan peak metamorphic conditions (T = 450–550°C, P = 0.5–0.65 GPa) estimated by RING & RICHTER (1994) using garnet-biotite thermometry and plagioclase–biotite–garnet–muscovite barometry. In addition, the results of pseudosection modelling also agree very well with the observed mineral assemblages in the samples.

Introduction

The Variscan basement of the Eastern Alps (Figures 1a, b) is confined to the west and north by the Periadriatic (Giudicarie line and Pustertal line) fault system (SCHMIDT et al. 1989). In the southeast, small basement outcrops within the Cenozoic molasse deposits of the Po Plain occur. Most of the basement is comprised of monotonous quartzphyllites, which were pervasively affected by the Variscan metamorphic and tectonic overprint. Due to its now slightly tilted position, the basement shows a metamorphic gradient, which increases from southeast towards northwest (SASSI & SPIESS, 1993).

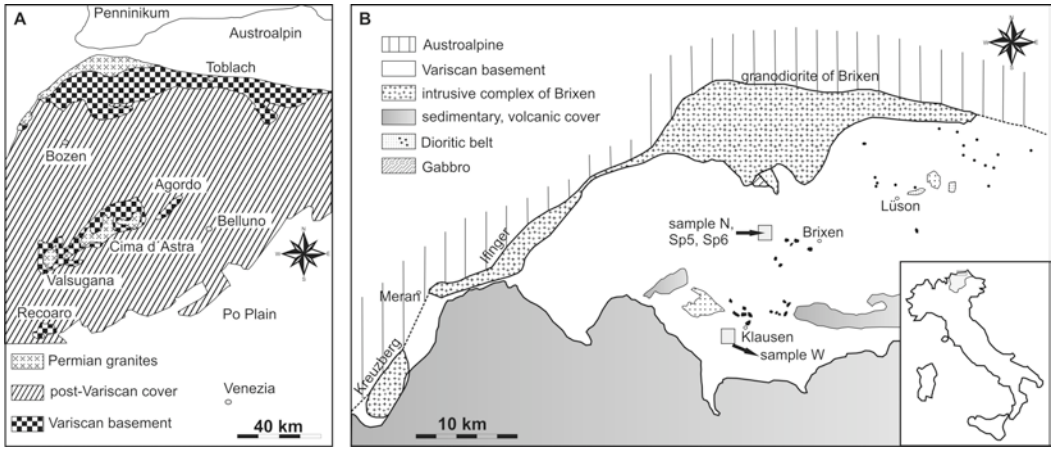

Figure 1

(a): Simplified geological map of the three major areas of the northern Southalpine crystalline basement in the Eastern Alps after SASSI & SPIESS (1993). (b): Simplified geological map of the study area showing the eastern Southalpine containing large Permian intrusions (from east to west: Kreuzberg-, Ifinger-, Brixen granites/granodiorites). The rectangle west of Brixen shows the location of the Spiluck samples SP6, SP5, N. The other rectangle to the south-west of Brixen, near Klausen, indicates the location of the Waidbruck sample W.

In the area of Toblach, the basement contains the mineral assemblage quartz + chlorite + white mica + albite and represents the lowest peak metamorphic conditions of the basement with temperatures of 350–400°C and a pressure of ca. 0.4 GPa. The metamorphic conditions increase towards the northwest and reach maximum P-T conditions in the area of Brixen/Bressanone. In this area the basement contains the mineral assemblage quartz + biotite + chlorite + white mica + garnet + albite + plagioclase and calculated P-T conditions based on conventional garnet-biotite thermometry and plagioclase–biotite–garnet–muscovite barometry yielded temperatures of 450–550°C and pressures of 0.5–0.65 GPa (RING & RICHTER, 1994).

In addition to the Variscan regional metamorphic overprint, the Permian Brixen pluton was emplaced during the Permian (280 Ma) into the country rocks of the Brixen quarzphyllite. Only a small part of the basement at the southern rim of the Brixen granodiorite was thermally affected by Permian contact metamorphism (PETRASCHEK, 1905; SANDER, 1906; SCOLARI & ZIRPOLI, 1970; WYHLIDAL et al., 2008). This led to the formation of a small, about 200 meters wide, contact aureole at the southern rim of the Brixen granodiorite near the village Franzensfeste/Fortezza (South-Tyrol, Italy).

Variscan ages of the Brixen quartzphyllite have been reported by several authors (DEL MORO et al., 1980; HAMMERSCHMIDT & STÖCKHERT, 1987; CAVAZZINI et al., 1991). Variscan age constrains indicate a two-stage development of this metamorphic event at 350 Ma and 320 Ma, which was first confirmed by microtextural observations by SASSI & ZIRPOLI (1968). DEL MORO et al. (1980) and CAVAZZINI et al. (1991) reported the Variscan metamorphic event at about 354 ± 10 Ma (Rb-Sr, whole rock-garnet-muscovite) and 347 ± 17 Ma (Rb-Sr, whole rock isochrone), which can be correlated with the initial flysch deposition at the Tournaisian-Viséan boundary (FRISCH & NEUBAUER, 1989). This age of 350 Ma is interpreted as the early regional heating (MELI, 2004). DEL MORO et al. (1984) also reported Rb-Sr, K-Ar and Ar-Ar ages of

white micas around 320 Ma and suggested that this age dates the thermal climax. These data are also in agreement with Rb-Sr and Ar-Ar ages by MELI (2004). HAMMERSCHMIDT & STÖCKHERT (1987) obtained Ar-Ar ages of 319 ± 6 Ma and 312 ± 6 Ma on muscovite which have been interpreted as cooling ages, consistent with the Rb-Sr mineral ages close to 300 Ma obtained by DEL MORO et al. (1984).
Since the conventional thermobarometric data from RING & RICHTER (1994) are the only quantitative P-T estimates from this area it was the aim of this study to provide modern thermobarometric constraints on the Variscan metamorphic event using multi-equilibrium methods and pseudosections. Therefore samples of the Brixen Quartzpyllite, which lack Permian contact metamorphism, were collected near Brixen (Spiluck/Spelonca, Waidbruck/Ponte Gardena) in South-Tyrol, Italy.

Analytical methods

About 30 thin sections of the Brixen quartzphyllite were investigated using the polarization microscope. A JEOL SUPERPROBE 8100 electron microprobe was used to analyze mineral compositions at the Institute of Mineralogy and Petrography at the University of Innsbruck. Analytical conditions were 15 kV acceleration voltage and 10 nA beam current. Natural mineral standards were used for calibration. The counting times for elements were 20 s for the peak and 10 s for the background. To prevent the volatilization of alkalis, feldspar and white mica were analyzed using a rastered beam whose size was depending on the crystal size. Bulk rock chemical analyses were done at the Institute for Earth Sciences, Department of Mineralogy and Petrology, University of Graz using a Bruker Pioneer S4 X-Ray fluorescence spectrometer. The samples were ground to a powder and prepared as fused pellets using a $LiBO_4$ flux.

Petrography

In the area of Brixen, the samples contain the mineral assemblage muscovite + chlorite + biotite (chloritized) + plagioclase + albite + garnet + quartz ± K-feldspar and accessory minerals such as zircon + apatite + ilmenite ± rutile ± monazite ± titanite. In the samples from Waidbruck, the assemblage is similar but plagioclase is rarely observed and no biotite occurs (Figure 2). Detrital zircons are besides monazite the main U-Pb mineral and frequently occur in the Brixen quartzphyllite. Garnet always occurs as porphyroblasts with a diameter of 1 mm up to 2 mm and often contains inclusions of quartz, ilmenite and apatite. The garnets are always continuously zoned. Muscovite and chlorite typically define the dominant Variscan foliation (Figure 2).

Bulk rock composition and mineral chemistry

Bulk rock compositions used for the calculations of the pseudosections are given in Table 1. The analysis given by SHAW (1956) represents an average of 18 published pelite compositions. The Al–index (=Al-3*(Na+K)–6.66*(Fe+Mg+Ca) indicates the degree of Al-saturation of a metapelite composition. Sample N therefore does not show a typical pelitic composition with respect to the Al-index. Generally, the sample from the area of Waidbruck (W) is quartz-poor, mica-rich and shows approximately 5 wt.% LOI in contrast to the mica-poor and quartz-rich samples (SP5, SP6, N) in the area of Brixen.

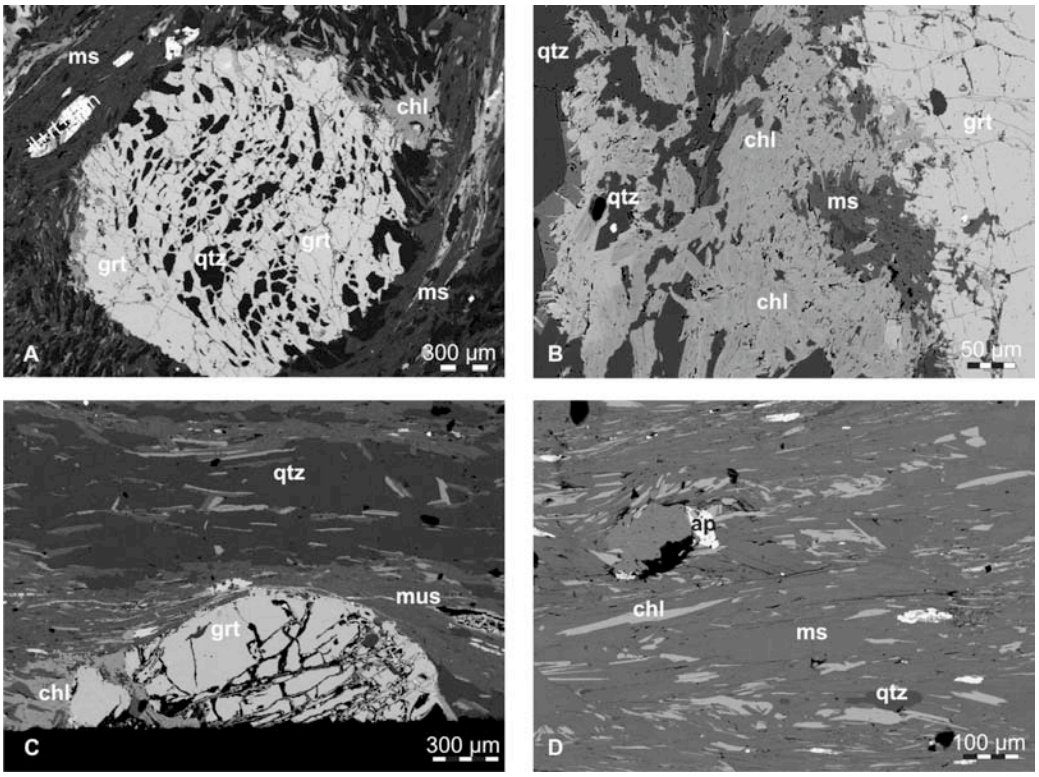

Figure 2
Backscattered electron (BSE) images of typical quartzphyllite samples from the northernmost Southalpine basement. (a): Typical garnet porphyroblast with quartz inclusions, in a matrix of chlorite, muscovite and aggregates of ilmenite + rutile + titanite from Waidbruck (sample W). (b): Close-up of the chlorite + muscovite + quartz matrix in a pressure shadow adjacent to garnet in sample W. (c): BSE picture of the basement in the area of Spiluck (sample SP5) showing a large fragment of a garnet porphyroblast in the typical quartz-poor and muscovite-rich matrix. (d): Close-up of the matrix of sample W.
Abbreviations: ms: muscovite; chl: chlorite; grt: garnet; qtz: quartz; ilm: ilmenite; rt: rutile; ttn: titanite; ap: apatite.

Garnet is mainly almandine-rich and always continuously zoned. The mole fraction of the almandine component increases from 60 mol.% in the core to 78 mol.% at the rim. Furthermore, the pyrope content also increases from core to rim (2.1 mol.% to 5 mol.%). In contrast, the contents of grossular (16–24 mol.%) and spessartine (0.1–10 mol.%) are decreasing towards the rim (Figure 3). This zonation reflects a prograde garnet growth during the Variscan metamorphic event (RING & RICHTER, 1994). Representative electron microprobe analyses of garnets are summarized in Table 2.

Plagioclase: Two chemical different plagioclase compositions, based on their anorthite contents, could be observed in the samples from the area of Brixen. One is an albitic plagioclase (X_{An} = 0–2 mol.%), and the second shows increasing X_{An} from 9–22 mol.%. Some plagioclase grains show an albite-rich core rimmed by oligoclase. This zonation most likely reflects prograde plagioclase growth during the Variscan metamorphic event (RING & RICHTER, 1994).

sample	N	SP5	SP6	W	Shaw (1956)
LOI	1.09	2.39	2.84	5.12	n.d
SiO_2	66.29	60.56	69.15	47.42	61.37
TiO_2	0.70	0.96	0.71	1.16	0.98
Al_2O_3	15.08	19.45	15.07	27.02	19.25
Fe_2O_3	6.71	7.50	4.93	8.35	7.68
MnO	0.18	0.20	0.05	0.14	0.07
MgO	1.41	1.09	1.42	2.11	2.03
CaO	2.03	1.13	0.36	0.03	0.46
Na_2O	4.47	1.71	0.46	0.59	1.30
K_2O	0.76	3.67	3.70	6.88	3.58
P_2O_5	0.24	0.15	0.13	0.09	n.d
Sum	98.95	98.80	98.81	98.91	96.72
Al-Index	-16.70	-6.67	-3.19	-4.20	-4.70
X Mg	0.71	0.78	0.64	0.67	0.66
K/(K+Na)	0.10	0.58	0.84	0.89	0.64

Table 1

Bulk rock compositions of the Brixen quartzphyllite.

The sample from SHAW (1956) represents an average composition of 18 published pelitic compositions. The Al–index (=Al-3(Na+K)-6.66*(Fe+Mg+Ca) indicates the degree of Al-saturation of a metapelite composition; n.d.: not detected.*

K-feldspar was occasionally observed in the matrix and contains only very little albite content (X_{Ab} <2 mol.%). Chemical compositions of all feldspars are shown in Figure 4. Representative electron microprobe analyses of feldspars are summarized in Table 3.

Muscovite is typically part of the main foliation. The chemical compositions of white micas lie along the muscovite–celadonite solid solution join and the Si content of muscovites ranges from 3.20 to 3.28 apfu with a mean value of 3.23 ± 0.03 (Figure 5). The amount of Na is below 0.01 apfu and no paragonite was observed in the samples. Representative electron microprobe analyses of white mica are summarized in Table 4.

Chlorite is also part of the main foliation and the X_{Mg} ranges between 0.35 and 0.42. Representative electron microprobe analyses of chlorite are summarized in Table 5.

Geothermobarometry

Multi-equilibrium thermobarometry was done using the program THERMOCALC v. 3.23 (POWELL & HOLLAND, 2001) and the thermodynamic dataset of HOLLAND & POWELL (1998). Calculation mode 2 (average pressure-temperature calculations) has been used for the P-T calculations. This approach utilizes calculation of all possible independent mineral reactions for a given set of minerals in order to obtain the equilibrium P-T conditions of the mineral assemblage.

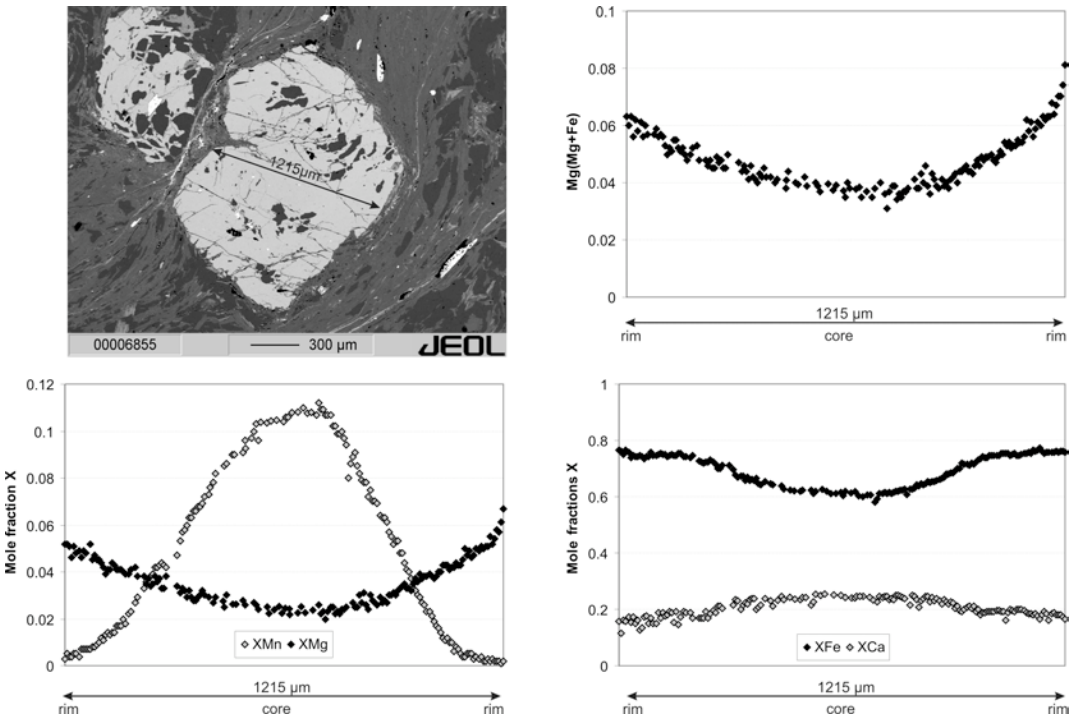

Figure 3

Compositional profile through a garnet porphyroblast illustrating the compositional variation of X_{Alm}, X_{Prp}, X_{Spes}, X_{grs} and Mg#; Mg/(Mg+Fe). Sample SP6.

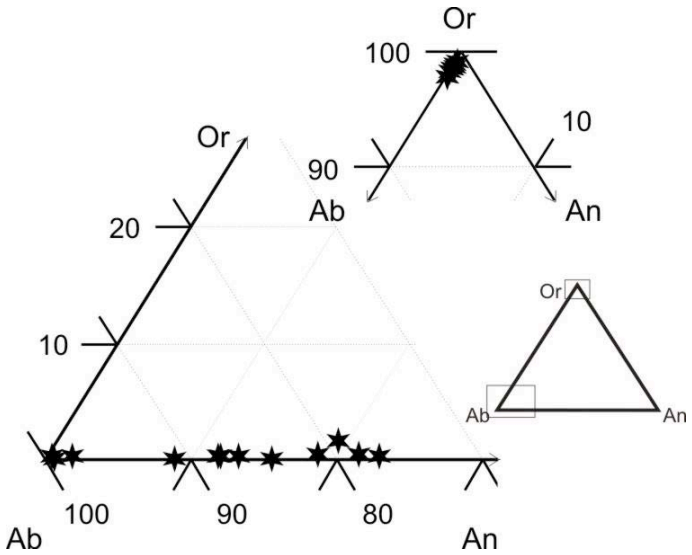

Figure 4

Triangle Ab-An-Or plot illustrating the chemical composition of plagioclase and K-feldspar, samples N, SP5 and SP6.

Sample	grt rim	grt rim	grt rim	grt core	grt core	grt core	grt rim	grt rim	grt rim
SiO_2	36.71	36.23	36.46	37.29	37.56	37.26	36.76	38.00	37.83
TiO_2	0.03	0.07	0.07	0.09	0.17	0.13	0.05	0.07	0.03
Al_2O_3	21.32	21.35	21.42	21.44	21.25	21.30	21.55	21.30	21.47
Fe_2O_3	0.56	2.08	0.93	0.57	n.c.	0.22	0.78	n.c.	n.c.
FeO	33.60	32.87	32.66	27.25	27.61	27.87	33.56	33.31	33.77
MnO	0.13	0.19	0.19	4.50	4.36	4.28	0.19	0.10	0.09
MgO	1.29	1.25	1.26	0.63	0.56	0.61	1.14	1.36	1.42
CaO	6.08	6.16	6.60	9.04	8.87	8.88	6.29	6.42	6.24
Na_2O	0.01	0.04	0.03	0.03	0.03	n.d.	0.01	n.d.	n.d.
K_2O	0.01	n.d.	n.d.	n.d.	0.01	n.d.	0.03	n.d.	0.02
Total	99.73	100.23	99.62	100.85	100.42	100.54	100.36	100.56	100.87
Si	2.968	2.921	2.949	2.973	3.007	2.981	2.955	3.040	3.017
Ti	0.002	0.004	0.004	0.005	0.010	0.008	0.003	0.004	0.002
Al	2.031	2.029	2.041	2.014	2.005	2.009	2.042	2.008	2.018
Fe^{3+}	0.034	0.126	0.056	0.035	n.c.	0.013	0.047	n.c.	n.c.
Fe^{2+}	2.271	2.217	2.209	1.817	1.849	1.865	2.256	2.229	2.253
Mn	0.009	0.013	0.013	0.304	0.296	0.290	0.013	0.007	0.006
Mg	0.155	0.151	0.151	0.075	0.066	0.073	0.136	0.162	0.169
Ca	0.526	0.532	0.572	0.772	0.761	0.761	0.542	0.551	0.534
Na	0.002	0.007	0.004	0.005	0.005	n.d.	0.002	n.d.	n.d.
K	0.001	n.d.	n.d.	n.d.	0.002	n.d.	0.003	n.d.	0.002
Grossular	0.159	0.115	0.162	0.239	0.249	0.244	0.158	0.185	0.179
Almandine	0.766	0.760	0.749	0.611	0.621	0.624	0.765	0.756	0.760
Pyrope	0.052	0.052	0.051	0.025	0.022	0.024	0.046	0.055	0.057
Spessartine	0.003	0.005	0.004	0.102	0.099	0.097	0.004	0.002	0.002
Andradite	0.017	0.065	0.029	0.017	n.c.	0.007	0.024	n.c.	n.c.
Ti-Al Grt	n.c.	n.c.	n.c.	n.c.	0.002	0.004	n.c.	0.002	n.c.
Na-Ti Grt	0.002	0.004	0.004	0.005	0.006	n.c.	0.003	n.c.	0.002
Al(IV)	0.033	0.079	0.051	0.027	n.c.	0.019	0.045	n.c.	n.c.
Al(VI)	1.999	1.951	1.990	1.987	2.005	1.990	1.997	2.008	2.018
xMg(Fe^{2+})	0.064	0.064	0.064	0.040	0.035	0.037	0.057	0.068	0.070
xMg(Fe^{tot})	0.063	0.060	0.063	0.039	0.035	0.037	0.056	0.068	0.070
Fe^{3+}/(Fe^{tot})	0.015	0.054	0.025	0.019	n.c.	0.007	0.021	n.c.	n.c.
xMg	0.052	0.052	0.051	0.025	0.022	0.024	0.046	0.055	0.057
$xFe^{(2+)}$	0.766	0.759	0.749	0.611	0.621	0.624	0.764	0.756	0.760
xCa	0.177	0.182	0.194	0.260	0.255	0.255	0.184	0.187	0.180
xMn	0.003	0.005	0.004	0.102	0.099	0.097	0.004	0.002	0.002

Table 2

Representative electron microprobe analyses of garnet.

The garnet analyses are from sample SP6. Formulae were calculated on the basis of 12 oxygens and 8 cations using the program NORM Version 4.0 (ULMER, 1993); Fe^{3+} was calculated according to charge balance considerations; n.d.: not detected; n.c.: not calculated.

Sample	kfs 1	kfs 2	kfs 3	ab 1	ab 2	pl 1	pl 2	pl 3
SiO_2	65.26	65.94	65.19	68.75	69.71	63.70	64.67	66.32
TiO_2	n.d.	n.d.	n.d.	n.d.	n.d.	n.d.	0.01	0.02
Al_2O_3	17.81	17.72	17.66	19.73	18.98	22.82	22.74	22.01
Fe_2O_3	n.d.	n.d.	n.d.	0.19	0.13	0.06	n.d.	n.d.
FeO	0.39	0.34	0.05	n.d.	n.d.	n.d.	0.12	0.07
MnO	n.d.	0.01	0.01	n.d.	n.d.	n.d.	0.01	0.02
MgO	n.d.	n.d.	n.d.	n.d.	0.01	n.d.	0.01	n.d.
CaO	n.d.	n.d.	n.d.	0.36	0.06	3.94	3.23	2.43
Na_2O	0.10	0.15	0.07	11.86	12.31	9.62	9.79	10.05
K_2O	16.67	16.36	16.90	0.10	0.07	0.11	0.05	0.07
Total	100.24	100.52	99.87	100.99	101.28	100.25	100.63	100.99
Si	3.020	3.045	3.025	2.972	2.999	2.803	2.834	2.895
Ti	n.d.	n.d.	n.d.	n.d.	n.d.	n.d.	<0.001	0.001
Al	0.972	0.965	0.966	1.005	0.962	1.183	1.174	1.133
Fe^{3+}	n.d.	n.d.	n.d.	0.006	0.004	0.002	n.d.	n.d.
Fe^{2+}	0.015	0.013	0.002	n.d.	n.d.	n.d.	0.004	0.003
Mn	n.d.	0.001	<0.001	n.d.	n.d.	n.d.	<0.001	0.001
Mg	n.d.	n.d.	n.d.	n.d.	0.001	n.d.	0.001	n.d.
Ca	n.d.	n.d.	n.d.	0.017	0.003	0.186	0.152	0.114
Na	0.009	0.013	0.006	0.994	1.027	0.821	0.832	0.851
K	0.984	0.964	1.001	0.006	0.004	0.006	0.003	0.004
An	n.d.	n.d.	n.d.	0.016	0.002	0.184	0.154	0.118
Ab	0.009	0.013	0.006	0.978	0.994	0.811	0.843	0.879
Or	0.991	0.987	0.994	0.005	0.004	0.006	0.003	0.004

Table 3

Representative electron microprobe analyses of feldspar.

Kfs 1, ab 1 and pl 1 are feldspar analyses of sample N. Kfs 2, ab 2 and pl 2 are feldspar analyses of sample SP5. Kfs 3, and pl 3 are feldspar analyses of sample SP6. Formulae were calculated on the basis of 8 oxygens and 5 cations using the program NORM Version 4.0 (ULMER, 1993); Fe3+ was calculated according to charge balance considerations; n.d.: not detected.

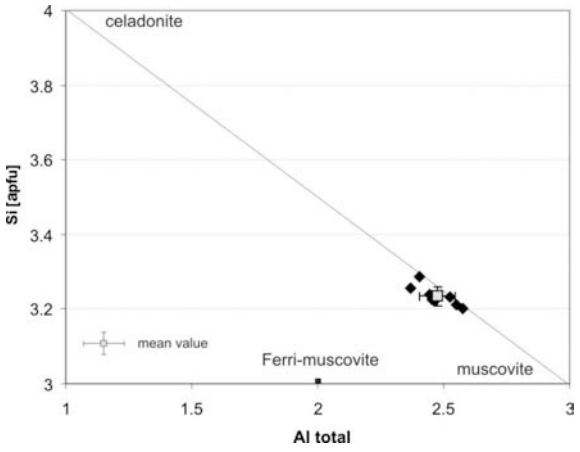

Figure 5

Si vs. Al total plot showing the chemical composition of muscovite, samples N, W, SP5 and SP6.

Sample	ms 1	ms 2	ms 3	ms 4	ms 5	ms 6	ms 7	ms 8
SiO_2	49.06	48.22	49.47	48.35	48.66	48.53	47.84	48.02
TiO2	0.26	0.27	0.29	0.33	0.34	0.29	0.22	0.26
Al_2O_3	30.30	31.13	30.72	33.00	32.77	31.07	31.68	31.20
Fe_2O_3	3.51	2.83	1.65	1.52	1.77	2.75	1.06	2.65
FeO	n.d.	n.d.	0.78	0.32	0.13	n.d.	1.16	0.65
MnO	n.d.	n.d.	n.d.	0.01	0.02	n.d.	0.03	0.05
MgO	1.89	1.65	1.71	1.14	1.30	1.68	1.09	1.25
CaO	n.d.	0.01	0.01	n.d.	0.01	n.d.	n.d.	n.d.
Na_2O	0.64	0.61	0.50	0.70	0.77	0.74	0.74	0.86
K_2O	9.54	9.60	9.99	9.74	9.61	9.41	9.69	9.57
F	n.d.	n.d.	n.d.	0.16	0.22	0.28	n.d.	n.d.
Cl	n.d.	n.d.	n.d.	0.02	n.d.	n.d.	n.d.	n.d.
H_2O	4.52	4.48	4.51	4.45	4.44	4.36	4.44	4.47
Total	99.70	98.79	99.62	99.72	100.03	99.10	97.94	98.98
F,Cl=O	n.d.	n.d.	n.d.	0.07	0.09	0.12	n.d.	n.d.
Total	99.70	98.79	99.62	99.65	99.94	98.98	97.94	98.98
Si	3.255	3.225	3.286	3.202	3.211	3.237	3.234	3.221
Ti	0.013	0.014	0.015	0.016	0.017	0.014	0.011	0.013
Al	2.370	2.454	2.405	2.576	2.549	2.443	2.524	2.467
Fe^{3+}	0.175	0.143	0.082	0.076	0.088	0.138	0.054	0.134
Fe^{2+}	n.d.	n.d.	0.043	0.018	0.007	n.d.	0.066	0.037
Mn	n.d.	n.d.	n.d.	<0.001	0.001	n.d.	0.002	0.003
Mg	0.187	0.165	0.169	0.112	0.128	0.167	0.110	0.125
Ca	n.d.	<0.001	0.001	n.d.	<0.001	n.d.	n.d.	n.d.
Na	0.082	0.079	0.064	0.090	0.099	0.096	0.097	0.112
K	0.807	0.819	0.846	0.823	0.809	0.801	0.835	0.819
F	n.d.	n.d.	n.d.	0.033	0.045	0.058	n.d.	n.d.
Cl	n.d.	n.d.	n.d.	0.002	n.d.	n.d.	n.d.	n.d.
H	2.000	2.000	2.000	1.965	1.954	1.942	2.000	2.000
xMg	0.516	0.536	0.574	0.546	0.573	0.548	0.480	0.424
# Cations	6.889	6.898	6.911	6.912	6.908	6.896	6.933	6.930

Table 4

Representative electron microprobe analyses of muscovite.

Ms 1 and ms 2 are muscovite analyses of sample N. Ms 3 and ms 4 is a muscovite analysis of sample SP5. Ms 5 and ms 6 are muscovite analyses of sample SP6. Ms 7 and ms 8 are muscovite analyses of sample W. Formulae of white micas were calculated on the basis of 11 oxygens and 6 cations + Na + K using the computer program NORM Version 4.0 (ULMER, 1993). Fe3+ was calculated according to charge balance considerations, n.d.: not detected.

Sample	chl 1	chl 2	chl 3	chl 4	chl 5	chl 6	chl 7	chl 8	chl 9
SiO_2	24.84	24.84	24.21	25.29	24.23	24.69	24.25	23.99	23.93
TiO_2	0.07	0.08	0.07	0.04	0.05	0.10	0.07	0.01	0.10
Al_2O_3	22.40	22.10	22.99	23.91	23.14	23.11	21.25	21.72	21.88
FeO	29.65	29.85	29.79	27.13	31.17	27.94	31.48	31.08	31.08
MnO	0.28	0.28	0.05	0.02	0.22	0.04	0.57	0.62	0.43
MgO	10.36	10.48	10.08	10.95	9.10	11.80	9.41	9.61	9.37
CaO	0.01	0.04	n.d.	0.01	n.d.	n.d.	n.d.	0.01	n.d.
Na_2O	n.d.	0.01	n.d.	0.04	n.d.	n.d.	n.d.	n.d.	n.d.
K_2O	0.02	0.04	n.d.	0.39	0.01	n.d.	n.d.	n.d.	0.01
H_2O	11.13	11.12	11.06	11.33	11.07	11.26	10.88	10.90	10.88
Total	98.76	98.83	98.25	99.10	99.00	98.94	97.92	97.94	97.67
Si	5.356	5.361	5.249	5.356	5.249	5.263	5.347	5.279	5.276
Ti	0.012	0.012	0.011	0.007	0.008	0.016	0.012	0.002	0.016
Al	5.690	5.620	5.874	5.966	5.907	5.804	5.521	5.633	5.684
Fe^{2+}	5.346	5.387	5.402	4.805	5.646	4.980	5.804	5.720	5.730
Mn	0.051	0.051	0.009	0.003	0.040	0.007	0.106	0.115	0.080
Mg	3.329	3.370	3.257	3.456	2.938	3.748	3.092	3.152	3.079
Ca	0.003	0.009	n.d.	0.002	n.d.	n.d.	n.d.	0.002	n.d.
Na	n.d.	0.006	n.d.	0.015	n.d.	n.d.	n.d.	n.d.	n.d.
K	0.005	0.010	n.d.	0.104	0.003	n.d.	n.d.	n.d.	n.d.
H	16.000	16.000	16.000	16.000	16.000	16.000	16.000	16.000	16.000
xMg #	0.384	0.385	0.376	0.418	0.342	0.429	0.348	0.355	0.350
Cations	19.791	19.825	19.802	19.714	19.791	19.819	19.881	19.903	19.865

Table 5

Representative electron microprobe analyses of chlorite

Chl 1 and chl 2 are chlorite analyses of sample N. Chl 3 and chl 4 are chlorite analyses of sample SP5. Chl 5 and chl 6 are chlorite analyses of sample SP6. Chl 7 to chl 9 are chlorite analyses of sample W. Formulae of chlorites were calculated on the basis of 36 oxygens using the computer program NORM Version 4.0 (ULMER, 1993). Fe^{3+} was calculated according to charge balance considerations, n.d.: not detected.

Activities of coexisting minerals (plagioclase, muscovite, chlorite, garnet) were computed using the program AX (POWELL & HOLLAND, 2001). All calculations were done with H_2O present and quartz in excess. Results for all samples yielded a temperature range from 519–551°C and pressures ranging from 0.53 to 0.59 GPa. These data are in good agreement with the peak metamorphic P-T conditions obtained by RING & RICHTER (1994) for the basement in the area of Brixen.

Pseudosection modelling: Equilibrium phase diagrams of natural samples, using the given bulk-rock compositions from Table 1 were calculated in the chemical system TiO_2–MnO–Na_2O–CaO–K_2O–FeO–MgO–Al_2O_3–SiO_2–H_2O. For the calculations, the software THERIAK–DOMINO (DE CAPITANI, 1994) with the thermodynamic database and solid solution models of HOLLAND & POWELL (2002, written communication) were used. All equilibrium phase diagrams were calculated over a P-T space of 0.45–0.65 GPa and 400–600°C to show the calculated stable mineral assemblages, which were then compared with the assemblages observed in the thin sections.

Results of pseudosection modelling

Sample SP6: This sample was collected in the area of Brixen (Spiluck) and is poor in Na_2O (0.46 wt.%). The X_{Mg} ratio is 0.64 and the ratio of K /(K+Na) is relatively high (0.84) compared to the average pelite composition. The equilibrium diagram calculated for the specific bulk–rock composition of sample SP6 is shown in Figure 6a. The grey area shows the observed mineral assemblage. The assemblage plagioclase + garnet + muscovite + chlorite + biotite + ilmenite + quartz + H_2O occurs in a large pressure stability field but only in a small temperature range and is limited towards higher temperatures by the staurolite-in isograd and towards lower temperatures by the stability limit of the assemblage garnet and biotite. Therefore, it can be deduced, that the observed mineral assemblage is stable at a pressure of 0.55 GPa in a temperature range of 540–570°C.

Sample SP5: Sample SP5 was also collected in the area of Brixen (Spiluck) and is rich in CaO and poor in MgO, therefore the Fe/(Fe+Mg) ratio of 0.78 is higher than the average metapelite composition of 0.66. Figure 6b shows the equilibrium phase diagram for the bulk rock composition of this sample. The grey shaded area points out the observed mineral assemblage plagioclase + garnet + muscovite + chlorite + biotite + ilmenite + quartz + H_2O and is limited towards higher temperatures again by the staurolite–in isograd and towards higher pressures by the stability field of the assemblage plagioclase + garnet + muscovite + paragonite + chlorite + biotite + ilmenite + quartz + H_2O. At lower temperatures the stability field of the observed assemblage plagioclase + garnet + muscovite + chlorite + biotite + ilmenite + quartz + H_2O is limited by the biotite-in isograd.

Sample N: This sample was also collected in the area of Brixen (main road from Brixen to Spiluck) and is enriched in Na_2O (4.47 wt.%) and extremely poor in K_2O (0.76 wt.%). Therefore the K/(K+Na) ratio is very low (0.10) and thus the sample has not a typical pelitic bulk rock composition in comparison to an average pelite composition. Furthermore CaO (2.03 wt.%) is enriched compared an average pelite composition (0.46 wt.%). In Figure 6c the equilibrium phase diagram for this specific bulk rock composition is shown. The grey shaded area indicates the observed mineral assemblage. The assemblage plagioclase + garnet + muscovite + chlorite + biotite + ilmenite + quartz + H_2O is stable over an extremely large stability field in P-T space. The upper temperature limit (≈ 540°C) is given by the stability of paragonite, which was not observed in the samples. Towards lower temperatures, the observed assemblage is limited by the garnet-in isograd.

Sample W: Sample W was collected near Waidbruck and contains the mineral assemblage garnet + muscovite + chlorite + ilmenite + quartz ± plagioclase. No biotite was observed and plagioclase is very rare. The sample W is very rich in K_2O and low in Na_2O with an extremely high K/(K+Na) ratio of 0.89. This composition is in agreement with the high content of white mica and the rare occurrence of plagioclase. The equilibrium phase diagram computed for this bulk composition is shown in Figure 6d. The observed mineral assemblage garnet + muscovite + chlorite + ilmenite + quartz ± plagioclase is highlighted by the grey area and is limited towards lower pressures by the stability field of the assemblage plagioclase + garnet + muscovite + chlorite + ilmenite + quartz + H_2O. The high temperature limit is represented by the biotite-in isograd. At lower temperatures, the stability of paragonite limits the observed mineral assemblage.

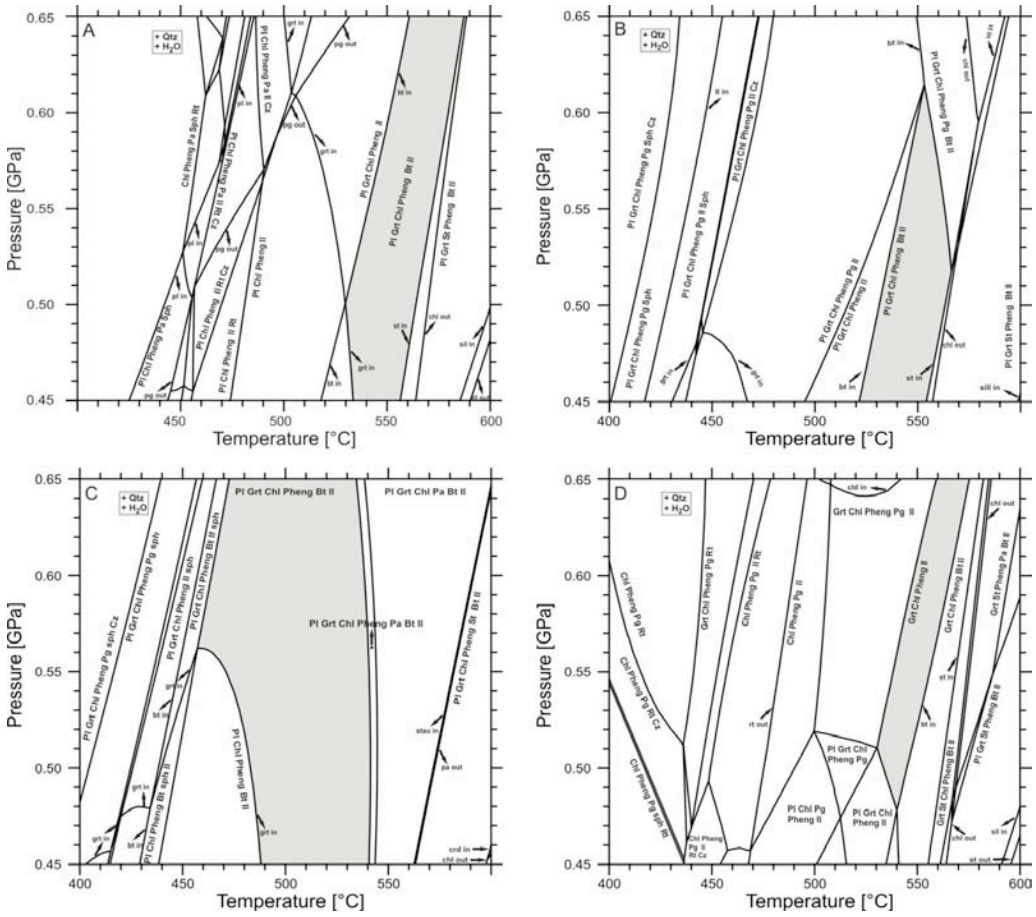

Figure 6

Equilibrium phase diagrams for bulk compositions SP6 (a), SP5 (b), N (c), and W (d). The diagrams were calculated in the chemical system TiMnNCKFMASH with the program DOMINO (DE CAPITANI, 1994) using the thermodynamic database of HOLLAND & POWELL (1998). Water is assumed to be present and quartz is stable in all phase fields. The grey areas represent the fields of the stable mineral assemblages which where observed in each sample. Samples which are collected in the area of Brixen (SP5, SP6, N) have the same mineral assemblage plagioclase (Pl) + garnet (Grt) + chlorite (Chl) + muscovite (Ms) + biotite (Bt) + ilmenite (Ilm) + quartz (Qtz). The Waidbruck (W) sample shows the mineral assemblage garnet (Grt) + chlorite (Chl) + muscovite (Ms) + ilmenite (Ilm) + quartz (Qtz) ± plagioclase (Pl).

Discussion

The Southalpine crystalline basement in the eastern Alps is south of the SAM (Southern Limit of Alpine Metamorphism, HOINKES et al. 1999) and is characterized by relatively low-grade Variscan metamorphism (greenschist-facies) and was injected by magmatic bodies during the Permian extensional event (SCHUSTER et al., 2001). The major intrusions show granitic/granodioritic compositions but small magmatic bodies of basic compositions also occur (DEL MORO & VISONÀ, 1982). The basement can be observed in the northern Southalpine domain in the following three different areas:

(1) In the area of the Sarntal-Brixen-Pustertal where the rocks of the basement are injected by the major intrusions of the Kreuzberg- Ifinger- and Brixen granodioritic bodies (SASSI & SPIESS, 1993). The basement shows high greenschist–facies (almandine–zone) overprint. At the rims of the plutons the Variscan metamorphic event is pervasively overprinted by Permian contact metamorphism (WYHLIDAL et al., 2008).

(2) In the area of Valsugana-Cima d´Asta-Agordo-Cereda. In this area the crystalline basement shows greenschist-facies (biotite–zone) metamorphism and is injected by the major intrusion of the Cima d´Asta granodioritic body and other minor intrusions (SASSI & SPIESS, 1993).

(3) The third area is the Recoaro area which only consists of low-grade (mainly chlorite–zone, lower geenschist–facies) metamorphic rocks.

MAZZOLI & SASSI (1988) described a regional metamorphic zonation and pointed out an increase in metamorphic grade from the East (Comelico area; chlorite–zone) to the West (Sarntal Alps; almandine–zone) and from the South (Recoaro area; chlorite–zone) to the North (Sarntal Alps; almandine–zone). Therefore, for this study, samples of the northernmost Southalpine crystalline basement in the eastern Alps were collected in the area of Brixen to calculate the maximum P-T conditions of the Variscan metamorphic event in the Southalpine domain. In samples from this area multi-equilibrium calculations yielded P-T conditions of 0.53–0.59 GPa and 521–551°C. This data are slightly higher but still in very good agreement with peak metamorphic conditions (T = 450–550°C, P = 0.5–0.65 GPa) reported by RING & RICHTER (1994). Pseudosection modelling has shown that the assemblage plagioclase + garnet + muscovite + chlorite + biotite + ilmenite + quartz + H_2O occurs in a large pressure stability field but only over a small temperature range (540–570°C) and is limited towards higher temperatures by the staurolite-in isograd and towards lower temperatures by the stability limit of garnet and biotite. The results of pseudosection modelling therefore agree very well with the observed mineral assemblages in the samples.

Acknowledgements

Financial support through FWF-project P-17878-N10 to P. T. is gratefully acknowledged. Bernhard Sartory is thanked for his assistance with the electron microprobe and Christoph Hauzenberger for his assistance with the XRF analysis.

References

CAVAZZINI, G., DEL MORO, A., SASSI, F. P. & ZIRPOLI, G. (1991): New data on the radiometic age of the Southalpine basement in the Eastern Alps. Geologia del Basamento Italiano. - Convegno in memoria di Tommaso Cocuzza, Siena 21-22 Marzo 1991, Abstract Volume.

DE CAPITANI, D. (1994): Gleichgewicht-Phasendiagramme: Theorie und Software. - Beiheft zum European Journal of Mineralogy 6, 48.

DEL MORO, A., SASSI, F. P. & ZIRPOLI, G. (1980): Preliminary results on the radiometric age of the Hercynian metamorphism in the South-Alpine basement of the Eastern Alps. - Neues Jahrbuch für Geologie und Paläontologie, Monatshefte 12, 707–718.

DEL MORO, A. & VISONA, D. (1982): The epiplutonic Hercynian complex of Bressanone (Brixen, Eastern Alps, Italy). Petrologic and radiometric data. - Neues Jahrbuch für Mineralogie, Abhandlungen 145, 66–85.

DEL MORO, A., SASSI, F. P. & ZIRPOLI, G. (1984): Acidic gneisses from Plan de Corones area, and chronological data on South-Alpine basement in Pusteria (Eastern Alps). - Memorie della Instituto Geologiche et Mineralogica Universita Padova 36, 403–412.

FRISCH, W. & NEUBAUER, F. (1989): Pre-Alpine terranes and tectonic zoning in the eastern Alps. - Geological Society of America Special Paper 230, 91–100.

HAMMERSCHMIDT, K. & STÖCKHERT, B. (1987): A K-Ar and $^{40}Ar/^{39}Ar$ study on white micas from Brixen quartzphyllite, Southern Alps. Evidence for argon loss at low temperatures. - Contributions to Mineralogy and Petrology 95, 393–406.

HOINKES, G., KOLLER, F., RANTITSCH, G., DACHS, E., HÖCK, V., NEUBAUER, F. & SCHUSTER, R. (1999): Alpine metamorphism of the Eastern Alps. - Schweizerische Mineralogische und Petographische Mitteilungen 79, 155–181.

HOLLAND, T. J. B. & POWELL, R. (1998): An internally-consistent thermodynamic data set for phases of petrological interest. - Journal of Metamorphic Geology 16, 309–343.

MAZZOLI, C. & SASSI, R. (1988): Caratteri del metamorfisimo ercinico nella fillade subalpina a ovest di Bressanone. - Memorie di Scienze Geologiche di Padova 40, 295–314.

MELI, S. (2004): Rb-Sr and $^{40}Ar/^{39}Ar$ age constraints on the Variscan metamorphism recorded by Ordovician acidic metavolcanic rocks in the Eastern Southalpine basement. - Rendiconti Lincei 9, 205-223.

PETRASCHEK, W. (1905): Über Gesteine der Brixener Masse und ihre Randbildungen. - Jahrbuch der Kaiserlich-Königlichen Geologischen Reichsanstalt 54, 47–74.

POWELL, R. & HOLLAND, T. J. B. (2001): Course notes for the THERMOCALC Workshop 2001: Calculating Metamorphic Phase Equilibria (on CD-ROM).

RING, U. & RICHTER, C. (1994): The Variscan structural and metamorphic evolution of the eastern Southalpine basement. - Journal of the Geological Society of London 151, 755–766.

SANDER, B. (1906): Geologische Beschreibung des Brixner Granits. - Jahrbuch der Kaiserlich-Königlichen Geologischen Reichsanstalt 56, 707–744.

SASSI, F. P. & SPIESS, R. (1993): The South Alpine metamorphic basement in the Eastern Alps. In: VON RAUMER, J. F. & NEUBAUER, F. (Eds): Pre-Mesozoic Geology in the Alps, Springer, Heidelberg, 599–607.

SASSI, F. P. & ZIPOLI, G. (1968): Il basamento cristallino di Recoaro. Studio petrografico. - Memorie della Società di Geologia Italiana 7, 227–245.

SCOLARI, A. & ZIPOLI, G. (1970): Fenomeni di metamorphismo di contatto nella fillade sudalpina indotti dal massiccio granitico di Bressanone (Alto Adige). - Memorie della Museo Tridentino Scienze Naturale 18, 173–222.

SCHMIDT, S. M., AEBLI, H. R., HELLER, F. & ZINGG, A. (1989): The role of the Periadriatic Linie in the tectonic evolution of the Alps. In: COWARD, M. P., DIETRICH, D. & PARK, R. G. (Eds) Alpine Tectonics. Geological Society of London Special Publication 45, 153–171.

SCHUSTER, R., SCHARBERT, S., ABART, R. & FRANK, W. (2001): Permo-Triassic extension and related HT/LP metamorphism in the Austroalpine Southalpine realm. - Mitteilungen der Gesellschaft für Geologie und Bergbaustudenten Österreich 45, 111-141.

SHAW, D. M. (1956): Geochemistry of pelite rocks III, major elements and general geochemistry. - Geological Society of America Bulletin 67, 919–934.

ULMER, P. (1993): Norm-program for cation and oxygen mineral norms. - Computer Library IKP-ETH, Zürich.

WYHLIDAL, S., THÖNY, W. F., TROPPER, P. & MAIR, V. (2008): Thermobarometry and experimental constrains of Permian contact metamorphism at the southern rim of the Brixen Granodiorite. - Journal of Alpine Geology 49, 118.

received: 06.04.2010
accepted: 17.05.2010